JOURNAL OF SOLID STATE CHEMISTRY **74**, 39–46 (1988)

The Luminescence of Ce^{3+}-Sensitized and Tb^{3+}-Activated Gadolinium Metaphosphates (GdP_3O_9–Ce,Tb)

H. S. KILIAAN, F. P. VAN HERWIJNEN, AND G. BLASSE

Physical Laboratory, State University of Utrecht, P.O. Box 80.000, 3508 TA Utrecht, The Netherlands

Received August 26, 1987; in revised form November 9, 1987

Energy transfer phenomena in rare-earth metaphosphate compounds have been investigated. For monoclinic GdP_3O_9–Ce,Tb (1%) at 300 K, it is shown that energy transfer does not take place from Ce^{3+} to Gd^{3+}, but from Gd^{3+} to Ce^{3+}. Moreover, no energy migration over the Gd^{3+} sublattice was observed. In the case of orthorhombic $La_{1-x}Gd_xP_3O_9$–Ce,Tb (1%) ($x \leq 0.68$) on the other hand, the excitation energy migrates from the Ce^{3+} ion to the Tb^{3+} traps via the Gd^{3+} sublattice. The energy migration over the Gd^{3+} ions is probably one-dimensional. In CeP_3O_9 rapid energy migration occurs over the Ce^{3+} ions. © 1988 Academic Press, Inc.

Introduction

de Hair showed in 1979 (*1*) that efficient lamp phosphors can be made, using energy transfer from a sensitizer *S* to an activator *A* via energy migration over the Gd^{3+} sublattice. We have investigated several of these systems (*2–6*). In this paper we will report on the luminescence of gadolinium metaphosphate (GdP_3O_9) doped with $S = Ce^{3+}$ and $A = Tb^{3+}$.

The rare-earth metaphosphates crystallize in two different crystal structures. According to Beucher (*7*) only the Gd^{3+} compound can be obtained with either crystal structure. The crystal structures have been unraveled by Hong (*8, 9*). The La- to Gd-metaphosphates have an orthorhombic crystal structure (*8*) and the Y and Gd to Lu compounds have a monoclinic crystal structure (*9*). We will refer to them as O and M, respectively.

In the M-structure, the RE^{3+} ions (*RE* = rare earth) are in octahedral coordination and form a three-dimensional sublattice. The nearest-neighbor distance is about 5.7 Å (see also Table I). There are four slightly different RE^{3+} crystallographic sites. Two of these sites have inversion symmetry, while the symmetry of the other two is low, viz. C_1 (*9*). Investigations by Agrawal and White (*10*) on GdP_3O_9–Eu^{3+} showed that the Eu^{3+} ion occupies a site symmetry which does not have pure inversion symmetry. More detailed investigations by Buijs and Blasse (*11*) reveal that there are at least two different sites for the Eu^{3+} ion. This is in agreement with the crystal structure data. For further details, refer to Ref. (*11*).

In the O-structure, the RE^{3+} ions are eightfold coordinated by oxygen and form a one-dimensional sublattice of zigzag chains along the *c* axis. The RE^{3+}–RE^{3+} distance

0022-4596/88 $3.00

TABLE I

CRYSTAL STRUCTURE DATA OF RARE-EARTH METAPHOSPHATES REP_3O_9

Compound[a]	Celparameters (Å)	RE^{3+}–RE^{3+} (Å)	Ref.
M-GdP_3O_9	a = 11.39 β = 96.8° b = 20.31 z = 12 c = 10.18	5.7 (2×) 6.0 (2×) 6.4 (2×) 6.6 (2×)	(*22*)
O-NdP_3O_9	a = 11.17 z = 4 b = 8.53 c = 7.28	4.2 (2×) 7.0 (8×) 7.3 (2×)	(*8*)

[a] O, orthorhombic phase; M, monoclinic phase.

in the chain is about 4.2 Å and the distance between two chains is about 7 Å.

The O-structure shows some similarity to $Li_6RE(BO_3)_3$ (*12*). In this borate the rare-earth ions form also a one-dimensional sublattice with RE^{3+}–RE^{3+} distance 4.2 Å in the chain and 6.9 Å between two chains (*12*). Energy migration processes in this system have been studied by Garapon *et al.* (*13*), Fu Wen Tian *et al.* (*14*), Buijs *et al.* (*15*), and by two of us (*5*). We will compare these two systems and make plausible that the energy migration in the Gd^{3+} sublattice of the O-structure is probably one-dimensional at room temperature and is comparable to that in $Li_6Gd(BO_3)_3$ (*13, 15*).

Experimental

The rare-earth metaphosphate compounds were prepared from intimate mixtures of RE_2O_3 and $(NH_4)_2HPO_4$ (15 mole% excess). These mixtures were fired for 1 hr at 400°C, 1 hr at 700°C, and 1 hr at 1000°C in a nitrogen atmosphere. Between the different firing stages the samples were reground. In Table II more information about the preparation is given.

We prepared the monoclinic form of $Gd_{0.98}Ce_{0.01}Tb_{0.01}P_3O_9$, orthorhombic $La_{0.98-x}Gd_xCe_{0.01}Tb_{0.01}P_3O_9$ ($x \leq 0.68$), and $Ce_{0.99}Tb_{0.01}P_3O_9$. The polycrystalline powders were checked by X-ray powder diffraction.

The instrumentation for the measurements of the luminescence has been described elsewhere (*3*).

Results and Discussion

1. Preparation

We prepared orthorhombic $La_{0.98-x}Gd_xCe_{0.01}Tb_{0.01}P_3O_9$ with $x \leq 0.68$. Attempts to prepare orthorhombic samples with $x > 0.68$ using different final heating temperatures, ranging from 600 to 850°C, and 1 hr or longer firing times (up to several days) were unsuccessful and resulted in mixtures of orthorhombic and monoclinic phases. This is surprising, because Beucher (*7*) reported the existence of GdP_3O_9 in the orthorhombic as well as in the monoclinic phase. The phase transition from orthorhombic to monoclinic takes place at about 850°C. Agrawal and Hummel (*16*) reported the same transition, but at 750°C. However, they were not able to identify their samples, which were held for 400 hr beneath the transition temperature. Moreover, Buijs and Blasse (*11*) were able, for the first time,

TABLE II

FIRING CONDITIONS FOR THE SYSTEM $(La,Gd)P_3O_9$: Ce,Tb

$La_{0.98-x}Gd_xCe_{0.01}Tb_{0.01}P_3O_9$	Firing temperature (°C)	Firing time (hr)	Result[a]
$0 \leq x \leq 0.68$	400 700 1000	1 1 1	O
$x > 0.68$	400 700 1000	1 1 1	O + M
$x = 0.98$	400 700 1000	1 1 1	M
$x = 0.98$	400 700 700–800	1 1 ≈100	O + M

[a] O, orthorhombic phase; M, monoclinic phase.

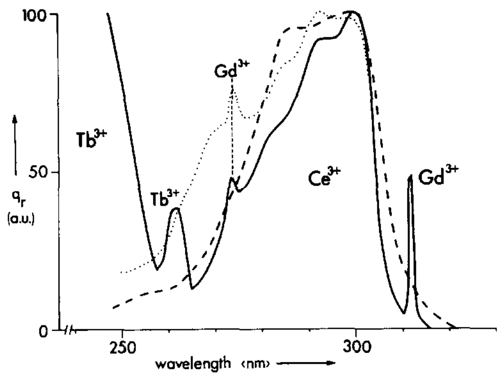

FIG. 1. Excitation spectra at LHeT of the Tb^{3+} $^5D_4$ emission (—), the Ce^{3+} emission (λ_{em} = 360 nm) (---), and the Ce^{3+} emission (λ_{em} = 325 nm) (. . .) in GdP_3O_9–Ce,Tb; q_r gives the relative quantum output in arbitrary units (a.u.).

to prepare orthorhombic as well as monoclinic EuP_3O_9. The total luminescence output of all the samples is high, so we will neglect the possibility of a considerable amount of nonradiative losses.

2. GdP_3O_9–Ce,Tb (M-Phase)

In Fig. 1 the excitation spectrum of the Tb^{3+} $^5D_4$ emission (λ_{em} = 542 nm) is plotted (solid curve) for liquid helium temperature (LHeT). We observe the following features:

(i) Lines at 312 and 274 nm, the Gd^{3+} $^8S_{7/2}$ to ^6P and ^6I transitions, respectively.

(ii) A broad band with its maximum at about 300 nm which is ascribed to the 4*f* to 5*d* transition on Ce^{3+}. This band is also present in the excitation spectrum of the Ce^{3+} emission (λ_{em} = 360 nm) which is also given in Fig. 1. The asymmetrical form of the band indicates that we are dealing with several overlapping transitions. There are two possibilities: (a) the transition are from the ground level $^2F_{5/2}$, to several components of the 5*d* state; (b) the observed transitions take place on Ce^{3+} ions on different crystallographic sites. At this stage, no decision can be made.

(iii) A band at about 263 nm and the onset of another excitation band, the maximum of which is outside the spectral region of the instrument. They do not occur in the excitation spectrum of the Ce^{3+} emission and are ascribed to $4f^8 \rightarrow 4f^75d$ transitions on Tb^{3+}. The weaker one is ascribed to the spin-forbidden component (transition to ^9D crystal-field component, Ref. (*17*)). The spin-allowed one is expected at about 6000 cm^{-1} higher energy (*17*), i.e., at about 230 nm. The spin-allowed one should also be at some 12,000 cm^{-1} higher energy than the Ce^{3+} excitation band (*18*), which places it at about 220 nm. Actually the diffuse reflection spectrum shows a band in this region. The onset is only a tail of this band, the spectrofluorometer being incapable of measuring at shorter wavelengths due to the use of a xenon lamp.

Upon excitation into the Ce^{3+} band (λ_{exc} = 300 nm) at LHeT, we observe Gd^{3+}, Tb^{3+}, and Ce^{3+} emission (see Fig. 2):

(i) The line emission at 312 nm is the Gd^{3+} ^6P to $^8S_{7/2}$ transition.

(ii) The other lines at about 380, 440, and 540 nm are the well-known Tb^{3+} transition from the $^5D_3$ and $^5D_4$ levels to the ground multiplet ^7F_J.

(iii) The two bands with $\lambda_{max} \approx$ 325 and 350 nm (the energy difference is about 2000

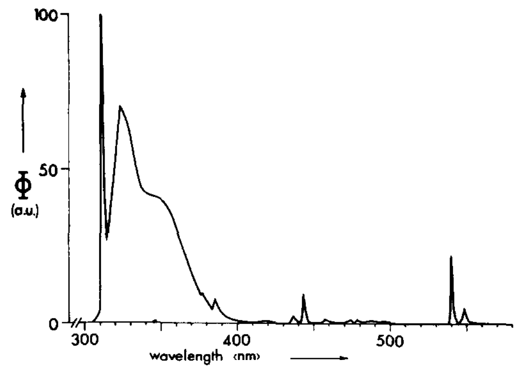

FIG. 2. Emission spectrum of GdP_3O_9–Ce,Tb upon excitation into the Ce^{3+} ion (λ_{exc} = 300 nm) at LHeT; Φ gives the spectral radiant power per constant wavelength interval in arbitrary units (a.u.).

cm^{-1}) are Ce^{3+} $5d$ to $4f$ transitions. At first sight these two bands can be considered to be transitions from the lowest $5d$ level to $^2F_{5/2}$ and $^2F_{7/2}$, respectively, but the excitation spectra of these two emissions point to another possibility. In Fig. 1, both excitation spectra are given. The two excitation spectra are clearly different, so that we have to assume that the two emission bands contain different contributions from Ce^{3+} ions on different crystallographic sites. This is in line with the crystal structure of this modification (*9*).

At room temperature (RT), only Ce^{3+} emission and a few percent of Tb^{3+} emission are observed upon excitation into the Ce^{3+} ion (λ_{max} = 300 nm). The emission spectra indicate that excitation into the Ce^{3+} ion is not followed by energy transfer to Gd^{3+}, but by radiative emission. This can be seen directly from the calculation of the critical distance R_c for energy transfer from Ce^{3+} to Gd^{3+}. Under dipole–dipole interaction, R_c can be calculated in the familiar way (*19*):

$$R_c^6 = 0.6 \times 10^{28} \cdot Q_{RE^{3+}} \cdot E^{-4} \cdot \mathrm{SO}. \quad (1)$$

The absorption cross section of the RE^{3+} ion, $Q_{RE^{3+}}$, in the case of energy transfer to Gd^{3+}, amounts to 5×10^{-23} cm^2 eV (*20*), and the experimental spectral overlap is SO ≈ 0.2 eV^{-1}. We obtain $R_c \approx 2.5$ Å.

Since in this crystal structure the shortest RE^{3+}–RE^{3+} distance is about 5.7 Å, a contribution by exchange interaction can be neglected. The absence of energy transfer from Ce^{3+} to Gd^{3+} in GdP_3O_9 is, therefore, corroborated by theory, so that the Ce^{3+} ions and Gd^{3+} ions are "isolated" from each other. The presence of Gd^{3+} emission in the 4.2 K emission spectrum is due to direct Gd^{3+} excitation as can be shown by shifting the excitation wavelength. At 300 K this emission is quenched due to energy transfer from Gd^{3+} to Ce^{3+} (*3*). At this temperature there is a reasonable spectral overlap between the Gd^{3+} emission and the Ce^{3+} absorption spectrum. The critical distance R_c for this back transfer is calculated using Formula (1), assuming dipole–dipole interaction. The absorption cross section $Q_{RE^{3+}}$ = $Q_{CE^{3+}}$ is large, since we are dealing with an allowed electric–dipole transition. With $Q_{CE^{3+}} \approx 5 \times 10^{-18}$ cm^2 eV (*20*) and an experimental spectral overlap SO ≈ 0.6 eV^{-1}, we find that R_c for the Gd^{3+}–Ce^{3+} transfer is about 20 Å.

Having discussed the $Ce^{3+} \leftrightarrow Gd^{3+}$ transfers, we turn now to a discussion of the transfer to the activator Tb^{3+}.

At RT, the Gd^{3+} emission is not observable due to back transfer to Ce^{3+}. Therefore, we prepared a sample without Ce^{3+}: $Gd_{0.99}Tb_{0.01}P_3O_9$. Upon excitation into the Gd^{3+} ^6I lines ($\lambda_{exc} \approx 276$ nm) we observe about 80% Gd^{3+} emission and about 20% Tb^{3+} emission. This intensity ratio points to a strongly hampered or even complete absence of energy migration over the Gd^{3+} sublattice.

By selective excitation into the higher ^6P levels of the Gd^{3+} ion we measured the Gd^{3+} decay at RT. The decay curve is single exponential with a decay time of 5 msec. This is a value which must be equal to or near the radiative decay time of the Gd^{3+} ion. Energy migration over the Gd^{3+} sublattice to traps is, therefore, practically absent. The critical distance for energy transfer between Gd^{3+} ions is then smaller than 5.7 Å in agreement with earlier results on other systems (*2*). The 20% of Tb^{3+} emission in the emission spectrum upon Gd^{3+} excitation is partly due to direct Tb^{3+} excitation and partly to one-step Gd^{3+}–Tb^{3+} transfer (see below).

In addition to a strong Gd^{3+} $^6P_{7/2}$ to $^8S_{7/2}$ emission ($\lambda_{max} \approx 311$ nm) we observe also weak emission lines at 305, 316, and 323 nm. The former is ascribed to the Gd^{3+} $^6P_{5/2}$–$^8S_{7/2}$ transition, while the latter two are cooperative vibronic Gd^{3+} emissions, due to coupling with the asymmetrical

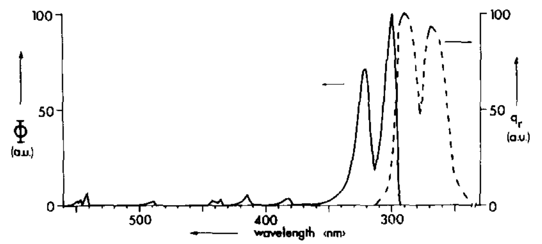

FIG. 3. Luminescence spectra of LaP_3O_9–Ce,Tb (both 1 at%) at LHeT. Right-hand side: Excitation spectrum of the Tb^{3+} $^5D_4$ emission, λ_{em} = 542 nm. Left-hand side: Emission spectrum upon excitation into the Ce^{3+} ion (λ_{exc} = 325 nm).

bending and stretching vibration modes of the surrounding phosphate groups.

3. *(La,Gd)P_3O_9–Ce,Tb (O-Phase)*

3.1. $La_{0.98}Ce_{0.01}Tb_{0.01}P_3O_9$. The excitation spectrum of the Tb^{3+} $^5D_4$ emission ($\lambda_{em} \approx$ 542 nm) at LHeT is given on the right-hand side of Fig. 3. The well-known Tb^{3+} excitation lines have been omitted. The spectrum consists of two broad bands at about 265 and 290 nm. The bands are due to $4f$ to $5d$ transitions on the Ce^{3+} ion.

Excitation into either band results in the emission spectrum given on the left-hand side of Fig. 3. It consists of Ce^{3+} emission and a few percent of Tb^{3+} emission. The Ce^{3+} emission is split into two bands with maxima at 305 and 325 nm (the energy difference being about 2000 cm^{-1}). The emission is from the lowest $5d$ level to the ground state levels $^2F_{5/2}$ (305 nm) and $^2F_{7/2}$ (325 nm). Excitation spectra of both Ce^{3+} emission bands result in identical spectra as shown in Fig. 3. Therefore, in contrast to the Ce^{3+} emission in GdP_3O_9–Ce,Tb (see Section 2), we conclude that the observed emission is from one Ce^{3+} center. This is in agreement with the crystal structure of, and the observations by Buijs and Blasse (*11*) on, LaP_3O_9–Eu^{3+}.

The RE^{3+} ions are eightfold coordinated (*9*). In first approximation, the eight coordination can be considered as cubic. This yields a crystal-field splitting in a higher t_2 and a lower e level. The coordination differs from cubic, because the RE^{3+} ion and its eight oxygen ligands form a bisdisphenoid dodecahedron. Therefore, the actual crystallographic site symmetry for the RE^{3+} ions in REP_3O_9 (O-phase) is lowered to C_2. This results in a further splitting of the cubic levels. From the excitation spectrum the splitting of the e level is found to amount to 2800 cm^{-1}.

The spectra indicate a small amount of energy transfer from Ce^{3+} to Tb^{3+}. This will be discussed below in more detail.

At RT, the situation is not markedly different. From the positions of the Ce^{3+} emission bands in LaP_3O_9 and the $^8S_{7/2}$ to ^6P transitions of Gd^{3+}, energy transfer from Ce^{3+} to Gd^{3+} in the O-phase is a probable process, because there will be a considerable spectral overlap. This will be discussed in the next paragraph.

3.2. $La_{0.98-x}Gd_xCe_{0.01}Tb_{0.01}P_3O_9$ (O-phase; $x \leq 0.68$). In the emission spectrum of a sample with x = 0.68, upon excitation into the Ce^{3+} ion, we observe, as in the case of monoclinic GdP_3O_9, cooperative vibronic Gd^{3+} emission at about 324 nm, superimposed on the lowest Ce^{3+} emission band.

Figure 4 shows the relative emission intensities of the Tb^{3+}, Gd^{3+} (^6P to $^8S_{7/2}$), and Ce^{3+} emissions as a function of the Gd^{3+} content at RT, upon excitation into the Ce^{3+} ion. Results for samples with $x > 0.68$ are not shown, because they are not single phase as discussed before (see Section 1).

The Ce^{3+} emission intensity decreases and the Tb^{3+} emission intensity increases linearly with increasing Gd^{3+} content. So, the introduction of Gd^{3+} into LaP_3O_9–Ce, Tb results in a more efficient energy transfer from Ce^{3+} to Tb^{3+}. The Ce^{3+} and Tb^{3+} concentrations are low (1 at %), so that direct energy transfer is strongly restricted. We conclude that the introduction of Gd^{3+} into LaP_3O_9–Ce,Tb makes energy transfer

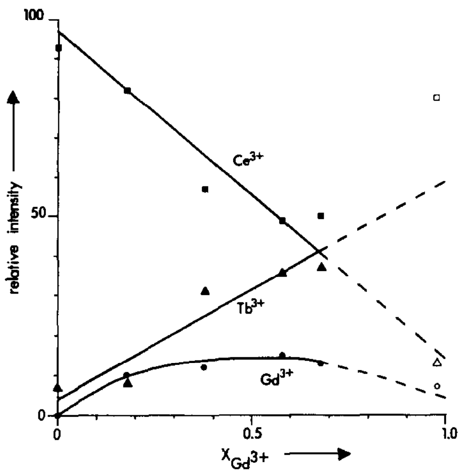

FIG. 4. The relative emission intensities of Ce^{3+} (■), Gd^{3+} (●), and Tb^{3+} (▲) as a function of the Gd^{3+} concentration x at room temperature for $La_{0.98-x}Gd_xCe_{0.01}Tb_{0.01}P_3O_9$ ($0 \leq x \leq 0.68$) and $Gd_{0.98}Ce_{0.01}Tb_{0.01}P_3O_9$ (M-phase) (□, ○, and △, respectively). Excitation is into the Ce^{3+} ion (λ_{exc} = 265 nm). An extrapolation of the values for the (La,Gd)P_3O_9 solid solution to x = 1 is also shown.

from Ce^{3+} to Tb^{3+} possible by migration over the Gd^{3+} sublattice (*1, 2*). This illustrates the important role of the Gd^{3+} ions. A critical distance for this transfer process, R_c, can be estimated in two ways. First, the decrease of the Ce^{3+} emission intensity, shown in Fig. 4, is given by:

$$I_{Ce^{3+}}(x) = I_{Ce^{3+}}(x = 0) \cdot (1 - x)^n, \quad (2)$$

where n is the number of Gd^{3+} neighbor sites to which Ce^{3+} can transfer its energy, and $(1 - x)$ gives the probability that such a site is not occupied by a Gd^{3+} ion. This implies that the Ce^{3+} ion has one or more Gd^{3+} neighbors, i.e., the n sites are within a sphere with radius R_c around the Ce^{3+} ion. Fitting the Ce^{3+} intensity curve to Eq. (2) gives $n = 1$. This value of n indicates that there is only one Gd^{3+} site within a sphere with radius R_c to which Ce^{3+} can transfer its excitation energy. In view of the structure data in Table I, R_c must be 4.2 Å.

Second, considering dipole–dipole interaction, R_c can be calculated with Eq. (1) (Section 2). With $Q_{RE^{3+}} = Q_{Gd^{3+}}$ and a spectral overlap SO of about 2.3 eV^{-1}, R_c is about 3.7 Å. This points to a small amount of exchange contribution in the transfer process.

The Gd^{3+} emission intensity reaches a maximum at about $x_{Gd^{3+}} = 0.6$. Unfortunately, we were not able to measure the relative emission intensity of Gd^{3+} for $0.68 \leq x \leq 1$ for reasons already discussed, and to estimate the critical distance for energy migration over the Gd^{3+} sublattice, R_{cr}. From the crystal structure data, the RE^{3+} ions have their nearest neighbors at about 4.2 Å and their next-nearest neighbors at 7 Å (see Table I). In general, the energy transfer between Gd^{3+} ions is restricted to about 5–6 Å, depending on the host lattice (*2*). Therefore, in view of Table I the energy migration in the orthorhombic system (La, Gd)P_3O_9–Ce,Tb is restricted to the nearest neighbors. The energy migration must be one-dimensional and the x_{cr} is expected to have a value of about 1.

Up to $x_{Gd^{3+}} = 0.68$, the system strongly resembles the system $Li_6(Y,Gd)(BO_3)_3$: Bi, Tb (*5*). In the latter system, the Gd^{3+} emission intensity reaches a maximum at about 0.5. At $x_{Gd^{3+}} = 1$, there still is Gd^{3+} emission observed; this indicates that the energy migration over the Gd^{3+} is one-dimensional. With increasing Gd^{3+} concentration the Bi^{3+} and Tb^{3+} emission intensities in that system are also decreasing and increasing linearly, respectively. Extrapolating the curves, shown in Fig. 4, to $x_{Gd^{3+}} = 1$ shows that there will still be some Gd^{3+} emission observed. This comparison suggests also that energy migration is one-dimensional. A study of orthorhombic GdP_3O_9–Ce,Tb is necessary to confirm this proposal.

The fact that the two systems resemble each other runs parallel to the observation that the energy migration over the Eu^{3+} sublattice in orthorhombic EuP_3O_9 and Li_6

$Eu(BO_3)_3$ is one-dimensional in both compounds (*11, 14, 15*).

Figure 4 has been extrapolated to $x = 0.98$ and the data for monoclinic GdP_3O_9–Ce,Tb have been included. This shows clearly that the luminescence output of the two modifications is strongly different. In the M-modification Ce^{3+} emission dominates, because the excitation energy cannot be transferred. In the O-modification the Ce^{3+} emission intensity is much lower due to the occurrence of $Ce^{3+} \rightarrow Gd^{3+}$ transfer. However, the transfer is far from complete because of the low number of nearest neighbors. Since $R_c \approx 4.2$ Å, the probability for Ce^{3+} emission is still half the probability for transfer to Gd^{3+}, due to the fact that there are only two nearest neighbors.

3.3. CeP_3O_9–Tb (orthorhombic). In view of the facts that we observe Ce^{3+} to Tb^{3+} transfer in these metaphosphates, and that the Ce^{3+} emission of the O-phase overlaps the corresponding excitation band at RT, we investigated CeP_3O_9–Tb with the aim of realizing energy migration over the Ce^{3+} ion to Tb^{3+}.

For $Ce_{0.99}Tb_{0.01}P_3O_9$ we found at RT mainly Ce^{3+} emission upon Ce^{3+} excitation, viz. 88% Ce^{3+} emission and 12% Tb^{3+} emission. For $La_{0.98}Ce_{0.01}Tb_{0.01}P_3O_9$ these values are 94 and 6%, respectively (see Fig. 4). At first sight this small difference seems to indicate that the physical processes in these samples are very similar. However, this is not the case as we will show now.

The transfer rate for Ce^{3+} to Tb^{3+} transfer by dipole–dipole interaction amounts to 14 P_r, where P_r is the radiative rate of the Ce^{3+} ion ($P_r \approx 5.10^7$ sec^{-1}). R_c for this transfer is 6.5 Å. These data are calculated, using Eq. (1) with SO ≈ 3 eV^{-1} and $Q_{Tb^{3+}} = 10^{-21}$ cm^2 eV (*20*).

The spectral data also makes possible the calculation of these data for $Ce^{3+} \rightarrow Ce^{3+}$ transfer by dipole–dipole interaction at 300 K. With SO ≈ 0.2 eV^{-1} and $Q_{Ce^{3+}} = 5.10^{-18}$ cm^2 eV, we find $R_c \approx 18$ Å and a transfer rate of $\geq 10^3$ P_r.

The latter data indicate rapid energy migration among the Ce^{3+} ions, which is probably one-dimensional. These data make it possible to calculate the Tb^{3+}/Ce^{3+} emission intensity ratio. For rapid migration: $I(Tb^{3+})/I(Ce^{3+}) = n_{Tb} \cdot P_{Ce \rightarrow Tb}/n_{Ce} \cdot P_r = 0.14$, to be compared with the experimental value of 0.14. This agreement is of course partly accidental, but shows the correctness of the description.

If no $Ce^{3+} \rightarrow Ce^{3+}$ transfer occurs, the intensity ratio can also be calculated. Using R_c and the crystallographic data, we find $I(Tb^{3+})/I(Ce^{3+}) = 0.06$. The experimental value for LaP_3O_9–Ce,Tb is also 0.06. These data show that rapid energy migration occurs in CeP_3O_9. A Tb^{3+} concentration of 1 at% is too low to trap the migrating energy efficiently. The data show that more than 10% is necessary. In a one-dimensional lattice the migration is then blocked, however.

For CeP_3O_9–Tb we observe also a weak Ce^{3+} emission band at 380 nm. Its excitation spectrum consists of a band at 305 nm and the Ce^{3+} excitation bands mentioned

TABLE III

ENERGY TRANSFER PROCESS IN GdP_3O_9 : Ce,Tb (M), (La,Gd)P_3O_9 : Ce,Tb (O), AND CeP_3O_9 : Tb (O) AT ROOM TEMPERATURE

	$R_c{}^a$		
	M-GdP_3O_9 : Ce,Tb	O-(La,Gd)P_3O_9 : Ce,Tb	O-CeP_3O_9 : Tb
Shortest RE–RE distance:	5.7	4.2	4.2
Ce → Gd	− ~2.5	+ ~4.2	
Gd → Ce	+ ~20	− ~0	
Ce → Tb	+ ~6.5	+ ~6.5	+ ~6.5
Gd → Gd	− <5.7	+ <4.2	
Ce → Ce			+ ~18

Note. All distances are in Å. R_c denotes the critical distance for the transfer process.
[a] −, No transfer observed; +, transfer observed.

above. The latter fact points to energy transfer from the intrinsic Ce^{3+} ions to a defect Ce^{3+} ion. The spectral overlap is very favorable, so that a small amount of defect Ce^{3+} ions is able to trap a certain amount of the migration excitation energy.

Conclusion

The metaphosphates doped with Ce^{3+} and Tb^{3+} ions show a large number of transfer processes. Table III summarizes the results at RT. It is clear that the metaphosphates are excellent hosts for luminescent ions, as observed for Sb^{3+} (*21*), Eu^{3+} (*11*), and now for Ce^{3+} and Tb^{3+}. The transfer rates are such that it is not possible to obtain an efficiently sensitized green phosphor with these host lattices.

Acknowledgments

The investigations were supported by the Netherlands Foundation for Chemical Research (SON) with financial aid from the Netherlands Foundation for Technical Research (STW).

References

1. J. Th. W. de Hair, J. Lumin. **18/19,** 797 (1979).
2. A. J. de Vries, H. S. Kiliaan, and G. Blasse, *J. Solid State Chem.* **65,** 190 (1986).
3. H. S. Kiliaan, A. Meijerink, and G. Blasse, *J. Lumin.* **35,** 155 (1986).
4. H. S. Kiliaan, J. F. A. K. Kotte, and G. Blasse, *J. Electrochem. Soc.* **134,** 2359 (1987).
5. H. S. Kiliaan and G. Blasse, *Mater. Chem. Phys.* **18,** 155 (1987).
6. H. S. Kiliaan, F. P. van Herwijnen, and G. Blasse, *Mater. Chem. Phys.* **18,** 155 (1987).
7. M. Beucher, "Les Elements des Terres Rares," Coll. No. 180, Vol. 1, p. 331 CNRS, Paris (1970).
8. H. Y.-P. Hong, *Acta Crystallogr. Ser. B* **30,** 468 (1974).
9. H. Y.-P. Hong, *Acta Crystallogr. B* **30,** 1857 (1974).
10. D. K. Agrawal and W. B. White, *J. Electrochem. Soc.* **133,** 1261 (1986).
11. M. Buijs and G. Blasse, to be published.
12. G. K. Abdullaev, Kh.S. Mamedov, P. F. Rza-Zade, Sh A. Guseinova, and G. G. Dzhafarov, *Russ. J. Inorg. Chem.* **22,** 1765 (1977).
13. C. T. Garapon, B. Jaquier, J. P. Chaminade, and C. Fouassier, *J. Lumin.* **34,** 211 (1985).
14. Fu Wen Tian, C. Fouassier, and P. Hagenmuller, *J. Phys. Solids* **48,** 245 (1987).
15. M. Buijs, J. I. Vree, and G. Blasse, *Chem. Phys. Lett.* **137,** 381 (1987).
16. D. K. Agrawal and F. A. Hummel, *J. Electrochem. Soc.* **127,** 1550 (1980).
17. J. L. Ryan and C. K. Jørgensen, *J. Phys. Chem.* **70,** 2845 (1966); G. Blasse and A. Bril, *Philips Res. Rep.* **22,** 481 (1967).
18. A. J. de Vries and G. Blasse, *Mater. Res. Bull.* **21,** 683 (1986).
19. D. L. Dexter, *J. Chem. Phys.* **21,** 836 (1953); G. Blasse, *Philips Res. Rep.* **24,** 131 (1969).
20. W. T. Carnall, *in* "Handbook on the Physics and Chemistry of Rare Earths" (K. A. Gschneidner, Jr. and L. Eyring, Eds.), Vol. 3, Chap. 24, North-Holland, Amsterdam (1979).
21. E. W. J. L. Oomen, R. C. M. Peters, W. M. A. Smit, and G. Blasse, *J. Solid State Chem.*, in press.
22. P. P. Melnikov, P. H. Komussarova, and T. A. Lymysova, *Izv. Akad. Nauk SSSR, Neorg. Mater.* **17,** 2110 (1981).